

Analysis of Proton Flux with Solar Wind Parameters, Symmetric (SYM) and Asymmetric (ASY) H-indices

A. Giri, A. D. Lama, B. Adhikari, S. Rimal and S. Khatri

Journal of Nepal Physical Society

Volume 8, Issue 3, December 2022

ISSN: 2392-473X (Print), 2738-9537 (Online)

Editor in Chief:

Dr. Hom Bahadur Baniya

Editorial Board Members:

Prof. Dr. Bhawani Datta Joshi

Dr. Sanju Shrestha

Dr. Niraj Dhital

Dr. Dinesh Acharya

Dr. Shashit Kumar Yadav

Dr. Rajesh Prakash Guragain

JNPS, 8 (3): 53-58 (2022)

DOI: <https://doi.org/10.3126/jnphysoc.v8i3.50727>

Published by:

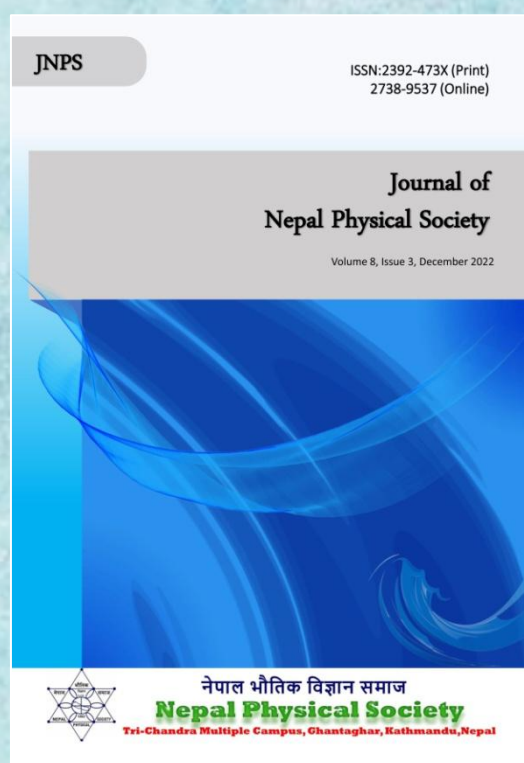
Nepal Physical Society

P.O. Box: 2934

Tri-Chandra Campus

Kathmandu, Nepal

Email: nps.editor@gmail.com





Analysis of Proton Flux with Solar Wind Parameters, Symmetric (SYM) and Asymmetric (ASY) H-indices

A. Giri¹, A. D. Lama¹, B. Adhikari^{1,2,*}, S. Rimal¹ and S. Khatri¹

¹Department of Physics, St. Xavier's College, Tribhuvan University, Kathmandu, Nepal

²Department of Physics, Patan Multiple College, Tribhuvan University, Nepal

*Corresponding Email: binod.adhi@gmail.com

Received: 16th July, 2022; Revised: 12th Oct., 2022; Accepted: 3rd Dec., 2022

ABSTRACT

After significant solar eruptions, protons are fired at extremely high speeds, sometimes reaching several thousand kilometer per second (km/s), resulting in solar radiation storms. Solar particle events can be found all around the heliosphere. The cross-correlation analysis along with time series analysis is used to look at how the solar wind and proton flux are related. The parameters used in this work are flux of Solar Energetic Protons (SEP) ranging from >10 MeV to >60 MeV along with speed, density, and pressure of the solar wind parameters. The findings indicate that proton flux (E>10 MeV) shows significant changes just before the storm while flux (E>30 MeV) and (E>60 MeV) doesn't correlate with solar parameters although during quiet day no significant changes were observed. These finding suggested that SEP can be used as precursor of CME driven storms.

Keywords: Coronal Mass Ejection (CME), Solar Proton Event (SPE), Solar Energetic Protons (SEP), Geomagnetic Storm (GMS), Cross-correlation.

INTRODUCTION

After significant solar eruptions, protons are fired at extremely high speeds, sometimes reaching several thousand kilometers per second (km/s), resulting in solar radiation storms. Solar Particle Electrons can be found all around the heliosphere. Onboard the Geostationary Operational Environmental Satellite Program (GOES) geostationary and National Oceanic and Atmospheric Administration (NOAA) polar orbiting satellites, Space Weather Prediction Centers' (SWPC) features high-energy proton detectors. SWPC's proton event threshold is 10 protons/cm²-s-sr at ≥ 10 MeV. The sporadic solar events, like solar flares, and Coronal Mass Ejection's (CME's) causes the dramatic enhancement of energetic fluxes near Earth. These solar energetic particle events occur quite frequently during maxima and very seldom during the minimum phase. Magnetosphere of planet acts as impenetrable obstacle for the continuous stream of plasma from the Sun (Burgess, 1995). If the CME's interplanetary

counterparts contain a strong southern component (Bz) of the Interplanetary Magnetic Field (IMF) in either the sheath behind the shock or the driving gas (magnetic cloud), they may cause Geomagnetic storms (GMSs) once they reach Earth's magnetosphere (Augusto *et al.*, 2018). Such complex interactions of earth's magnetic field and streams of plasmas from sun depends on various control parameters influencing the geomagnetic storms. When these eruptive events are sufficiently energetic to accelerate particles to relatively high energy, then they penetrate the Earth's magnetosphere and atmosphere (Koldobskiy *et al.*, 2021).

GMSs happens usually in three phases: the initial phase where an abrupt change in Disturbance Storm Time (Dst) can be seen also known as sudden commencement, the main phase when Dst assumes negative value and ends with minimum decrease and the recovery phase where Dst returns to its pre sudden commencement value. So Dst classifies GMSs as intense storm (peak Dst ≤ -100 nT), moderate storms (-100 nT <

peak Dst < -50 nT) and weak storms (peak Dst > -50 nT) (Gonzalez et al., 1994).

Reedy (1977) studied the proton fluxes emitted during the solar flares since the start of 1956 and a correlation between the solar flux and sunspot numbers. Kahler (1982) studied the correlations between solar energetic proton fluxes and related microwave burst parameters, the involvement of the huge flare syndrome. In their research, they suggested and tested a different theory for these relationships, the big flare syndrome (BFS), which claims that energetic flare events are statistically stronger in larger flares regardless of the specific physics. Qin et (2014) studied the variations in the inner radiation belt's trapped proton flux during solar cycles and observed that during the solar minimum, the area where the proton flux maxima advance westward at a faster pace each year. While the peak region moves southward during solar maximum, it moves more quickly in the reverse way during solar minimum. Pandya et al. (2021) issued the quantitative evaluation of protons during the September 2017 solar proton events. The higher level of solar proton flow population sustained for about two days, according to data from numerous spacecraft positioned in various parts of the Earth's magnetosphere.

Many academics are dedicating major theoretical and computational resources to understanding the proton flux of different energies coming towards the Earth. In this research we tried to cross-correlate different energies of proton fluxes with solar wind parameters and geomagnetic indices on intense storm and weak storm, to find out if proton flux can be used as precursor of geomagnetic storms or not.

DATASET AND METHODOLOGY

In this work, we have used space weather data measured during geomagnetic storm and quiet day of the solar cycle 24 provided by Omni web data source which is maintained by Space Physics Data Facility of NASA/Goddard Space Flight Centre

(https://omniweb.gsfc.nasa.gov/form/omni_min.html). These events were selected based on the Dst index, which is derived from a network of near-equatorial geomagnetic observatories. From the OMNI system, we selected data observation of interplanetary magnetic field (Bz in nT), Provisional Activity Indexes (ASY/H, SYM/H), Proton density (Nsw), Temperature (Tsw) and

Speed (Vsw) of solar wind and proton flux > 10 MeV, E > 30 MeV and E > 60 MeV which is acquired by GOES 13.

Cross-correlation analysis used to depict the relation between proton flux of different energies with other solar parameters for storm time and quiet day. Correlation is a statistical measure of degree to which 2 variables evolve in coordination with each other. If the variables change in the same direction they are said to be positively correlated. If the variable change in opposite direction, they are said to be negatively correlated. Cross correlation is a tool for finding out the degree of correlation between two time series, with its roots in statistics and signal processing (Marcq et al., 2010, Adhikari et al., 2017). It helps to estimate lag between signals, decipher other hidden signals within a signal, find periodicity/phase within a signal, and reveal underlying frequency content. Cross correlation analysis is a gateway to approaching other advanced analytical concepts like frequency filtering, Fourier analysis, and wavelet analysis. If we suppose two series say, $X = x_i$ and $Y = y_i, i = 0, 1, 2, \dots, N - 1$, the cross correlation between X and Y denoted by ρ_{zy} , at delay or lag (l) is defined as:

$$\rho_{xy}(l) = \frac{\sum_{i=0}^{N-1} [(x_i - \bar{x})(y_{i-l} - \bar{y})]}{\sqrt{\sum_{i=0}^{N-1} (x_i - \bar{x})^2} \sqrt{\sum_{i=0}^{N-1} (y_{i-l} - \bar{y})^2}} \dots \dots \dots (3.1)$$

where, \bar{x} is the mean of X and \bar{y} is the mean of Y.

The lag is the number of time periods that separate the two-time series. Equation 3.1 is termed as Pearson product-moment correlation coefficient or Normalized Cross Correlation Coefficient. If x_t and y_t are two time series, separated by l time units then the cross-correlation between the two-time series is equivalent to correlation between x_t and y_{t+l} . For purpose relevant to this work, we have set maximum lag to be the common range of time of available data. In this research, the cross-correlation proton flux of different energies of was observed with other parameters.

RESULTS AND DISCUSSION

During geomagnetic storms, the earth's magnetic field is disrupted. The sun and the magnetosphere are linked, resulting in several changes that occurs both in interplanetary space and terrestrial

environment on the ground (Gonzalez *et al.*, 1994). This section presents the time series analysis of plot proton fluxes of different

energies, solar parameters, and geomagnetic indices during solar storms of 15-19th March 2015 and quiet day of 13-18th May 2019.

Event 1: 15-19th March 2015

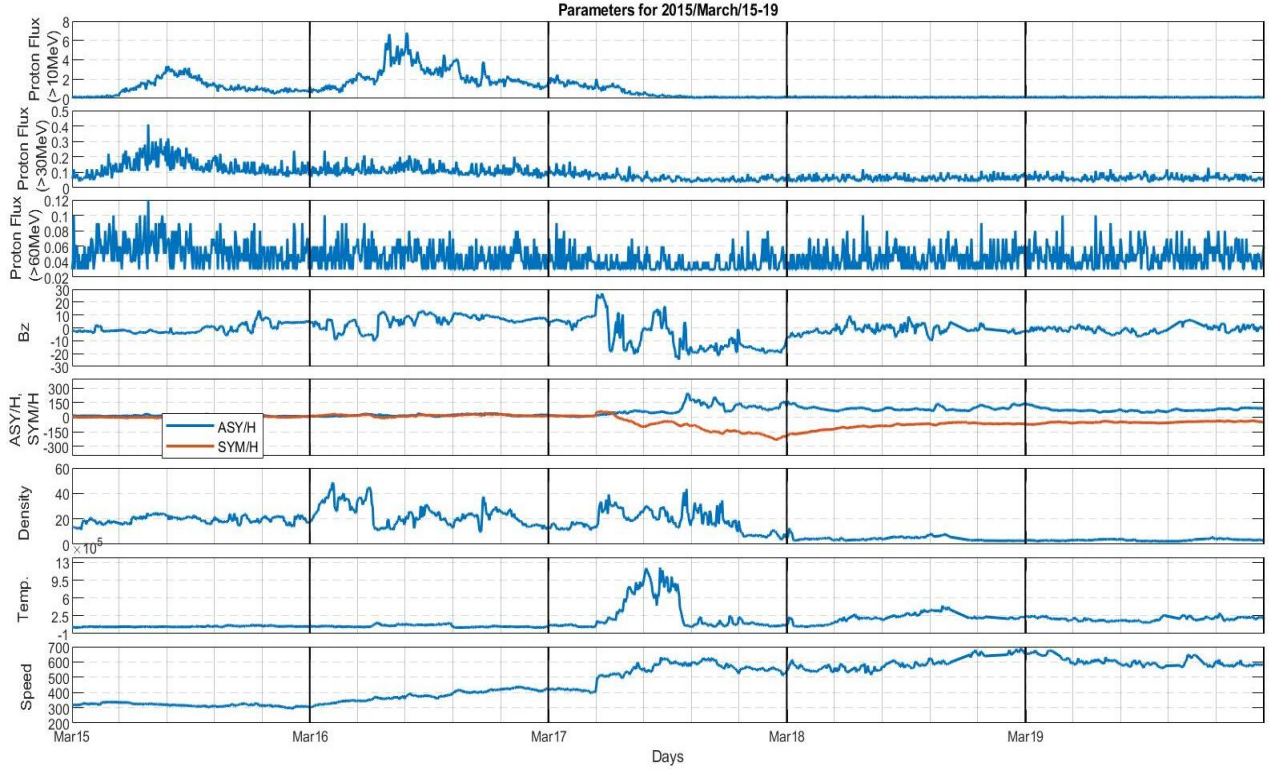


Fig. 1: The time series plot of proton flux $E > 10 \text{ MeV}$ ($\text{cm}^{-2}\text{S}^{-1}\text{Sr}^{-1}$) in first panel, $E > 30 \text{ MeV}$ in second panel and $E > 60 \text{ MeV}$ in third panel, interplanetary magnetic field (B_z in nT) fourth panel, Indexes (ASY/H, SYM/H) in fifth panel, Proton density (N_{sw} in n/cc) in sixth panel, Temperature (T_{sw} in Kelvin) in seventh panel, Flow speed (V_{sw} in km/sec) in eighth panel from top to bottom for Event-1 of 2015 March 15-19.

The top three panels of figure 1 depicts the value of proton flux for event 1 which shows increase in values of fluxes just before the main event day of March 17 which is St. Patrick’s Day. We expect this increase in proton flux is due to partial halo CME which was associated with C9.1/1F flare and series of type II/IV radio bursts (Wu *et al.*, 2016). After the commencement of storm, we can clearly see the value of proton fluxes decreases to minimum and remain low in recovery phase of storm validating the results of Oka *et al.* (2021).

In fourth and fifth panel, the shock produced by sudden storm commencement (SSC) at early hours of March 17 with a southward wind which intensified the storm (SYM-H dropped to $\sim -150\text{nT}$). A few hours later, storm recovered slightly (i.e. SYM-H dropped to $\sim -100\text{nT}$). Again, IMF turned southward due to strongly negative B_z

caused by second storm intensification with SYM-H = $\sim -250\text{nT}$. Wu *et al.* (2016) described the second storm intensification is due to southward magnetic cloud field. The magnetic cloud isn’t responsible for change in values of proton flux. Sixth and seventh panels show the changes in solar wind parameters, N_{sw} , T_{sw} and V_{sw} . On the other hand, the density reaching maximum of 50 n/cc few hours before the commencement of storm and dropping to lowest value of ~ 5 n/cc during the recovery phase. The temperature shows abrupt increase in value during the storm time of March 17 which is in accordance with previous researches. In the last panel we can see the value of solar wind velocity increasing abruptly during early hours of March 17 as the storm turns southward and goes on increasing which suggest Corotating Interaction Region (CIR) driven storm validating results of Matamba *et al.* (2018).

Event 2: 13-17th May 2019

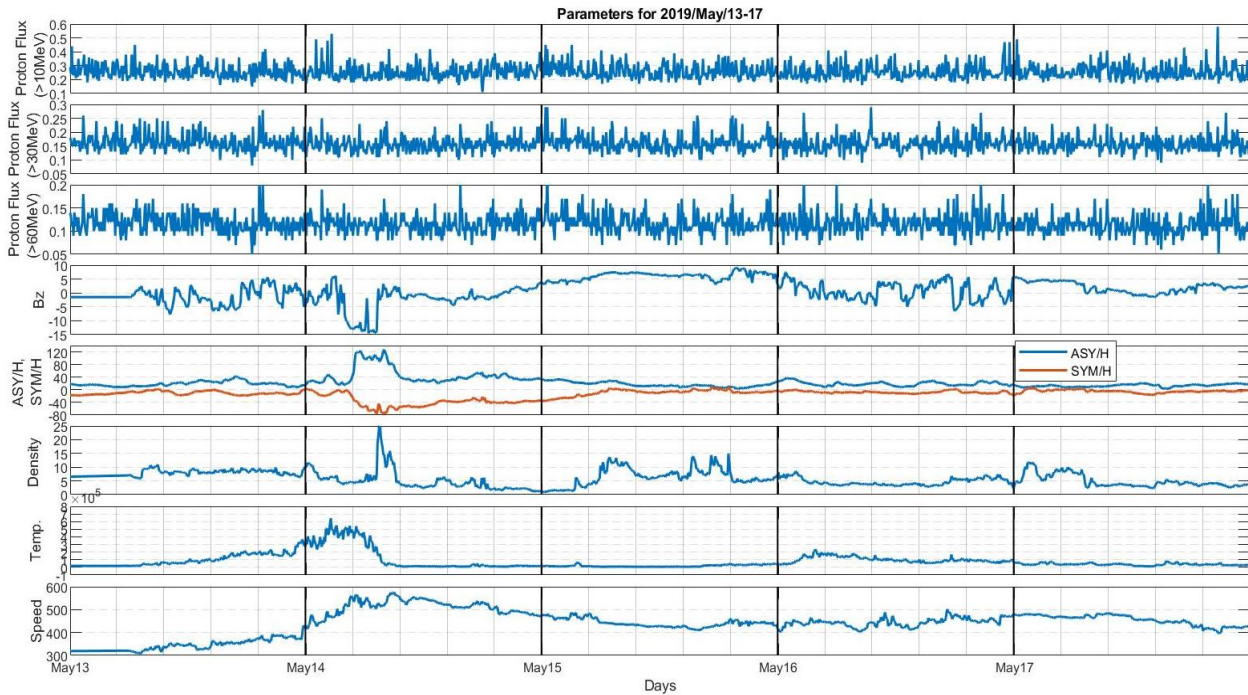


Fig. 2: The time series plot of proton flux $E > 10\text{MeV}$ ($\text{cm}^{-2}\text{S}^{-1}\text{Sr}^{-1}$) in first panel, $E > 30\text{MeV}$ in second panel and $E > 60\text{MeV}$ in third panel, interplanetary magnetic field (B_z in nT) fourth panel, Provisional Activity Indexes (ASY/H, SYM/H) in fifth panel, Proton density (N_{sw} in n/cc) in sixth panel, Temperature (T_{sw} in Kelvin) in seventh panel, Flow speed (V_{sw} in km/sec) in eighth panel from top to bottom for Event-2 of 2019 May 13-17.

Similarly, figure 2 describes variation of parameters for weak storm of 2019 May 16. Top three panels show fluctuation in proton flux and these values are very less ($\sim 0.2\text{-}0.6$ MeV) as compared to event one ($\sim 0\text{-}8$ MeV) suggesting proton flux might be used as precursor of geomagnetic storms induced by CMEs. In fourth panel, we can see the value of B_z starts at -1 nT for May 13, the value of B_z ends at -0.2 nT. In the next day the value of B_z hits the minimum value of -15 nT at 08:00 UT. The value of B_z then increases till the next day (May 15) and reaches the maximum value of 9 nT at 21:00 UT when storm changes from southward to northward direction. Again, B_z decreases to 3 nT at the end of May 17. In the fifth panel, we studied the variation of ASY/H and SYM/H which showed quiet obvious results for weak storm day on May 15, the first two weak CME events occurred with SYM-H = ~ -30 nT around early hours and of value -80 nT and dropped to ~ 0 nT with changing direction of solar wind till late hours of 16 May where third CME occurred with another southward solar storm.

Cross-Correlation:

First panel of figure 3 illustrates cross correlation between Proton flux ($E > 10$ MeV) with B_z Sky blue line, V_{sw} with Pink, N_{sw} with Yellow, T_{sw}

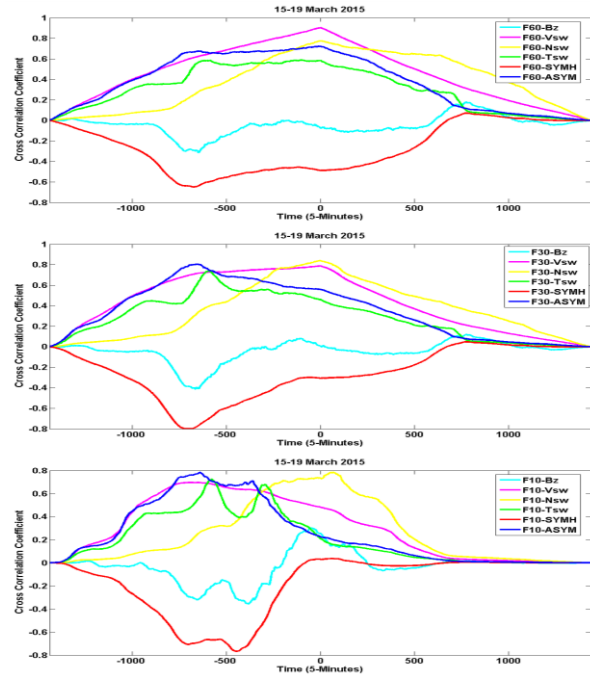


Fig. 3: Cross correlation between Proton flux ($E > 10$ MeV) with B_z , V_{sw} , N_{sw} , T_{sw} , SYMH and ASYH in first panel, Proton flux ($E > 30$ MeV) with B_z , V_{sw} , N_{sw} , T_{sw} , SYMH and ASYH in second panel, Proton flux ($E > 60$ MeV) with B_z , V_{sw} , N_{sw} , T_{sw} , SYMH and ASYH in third panel during Storm, 15-19 March, 2015.

with Green, SYMH with Red line and ASYH with blue line during Storm, 15-19 March, 2015. Similarly, second panel and third panel illustrates cross correlation with same line color code for flux ($E>30$ MeV) and flux ($E>60$ MeV) respectively. The x-axis represents time from 13 to 18 May 2019 with 5 minute resolution. While y-axis represents cross correlation coefficient from -0.8 to 1. All the proton fluxes have nearly average to good correlation with solar parameters but in case of Bz the correlation is insignificant while SYM/H has asymmetrical negative correlation with proton fluxes of different energy. The correlation between flux of different ranges and parameters follow different pattern during the storm.

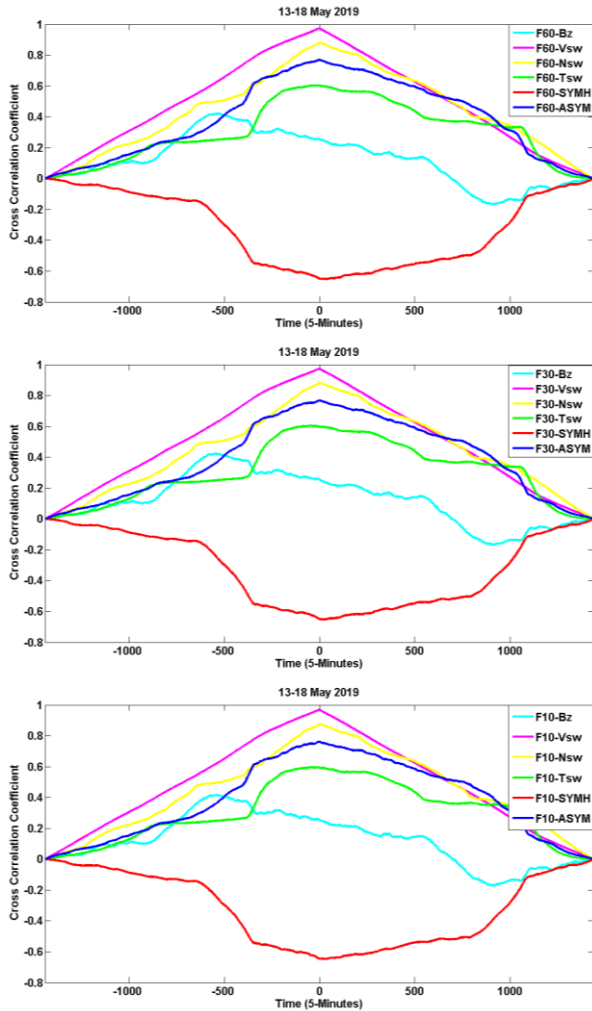


Fig. 4: Cross correlation between Proton flux ($E > 10$ MeV) with Bz, Vsw, Nsw, Tsw, SYMH and ASYH in first panel, Proton flux ($E>30$ MeV) with Bz, Vsw, Nsw, Tsw, SYMH and ASYH in second panel, Proton flux ($E>60$ MeV) with Bz, Vsw, Nsw, Tsw, SYMH and ASYH in third panel during Quiet Day, 13-18 May, 2019.

Similarly, the first panel of figure 4 illustrates cross correlation between Proton flux ($E > 10$ MeV) with Bz Sky blue line, Vsw with Pink, Nsw with Yellow, Tsw with Green, SYMH with Red line and ASYH with blue line during Storm, 15-19 March, 2015. The second panel and third panel illustrate cross correlation with same line color code for flux ($E>30$ MeV) and flux ($E>60$ MeV) respectively. Like case of event 1, the proton fluxes have nearly average to good correlation with all solar parameters except in case of Bz. Correlation of proton fluxes with Bz is insignificant and SYM/H has asymmetrical negative correlation with proton fluxes of different energies. The correlation between fluxes and parameters follows same pattern for the quiet event as there are no considerable fluctuations in proton fluxes of different energies which is in accordance with the time series analysis.

CONCLUSIONS

In this paper, we have analysed various solar wind parameters and geomagnetic indices with proton fluxes datasets for the two geomagnetic events selected. To study the response of proton flux distribution cross-correlation analysis was adopted. The finding of this research summarized as:

1. A good correlation, having a positive cross-correlation coefficient nearly 0.99 for proton flux with the solar wind velocity, >0.7 for solar and plasma density.
2. Proton fluxes are negatively correlated with SYM-H, this result suggested that decrease in SYM-H value isn't necessarily for solar proton event to occur while in case of ASY-H the correlation is nearly positive with low correlation coefficient but is insignificant.
3. As ASY/H has good correlation with proton fluxes so it can be recommended to use ASY/H index to predict solar proton events.
4. Our finding shows with long trend analysis we can use SEP can be used as precursor of CME driven storms and forecast space weather.

Thus, the findings suggested that proton fluxes show significant changes just before the storm. Moreover, the abrupt increase in proton flux observed more on ICME storm rather than weak storms. Hence, this research suggested that SEP can be used as precursor of CME driven storms. However, for more defined way to use SEP as precursor of CME driven storm, more events are needed to be analysed.

ACKNOWLEDGEMENT

The author would like to acknowledge the space weather data archive of the High Resolution OMNI (HRO) of NASA, https://omniweb.gsfc.nasa.gov/form/omni_min.html and the International Service of Geomagnetic Indices (ISGI), http://isgi.unistra.fr/data_download.php

REFERENCES

- [1] Adhikari, B.; Sapkota, N.; Baruwal, P.; Chapagain, N. P.; & Braga, C. R. Impacts on cosmic-ray intensity observed during geomagnetic disturbances. *Solar Physics*, **292**(10): 1-18 (2017).
- [2] Adhikari, B.; Dahal, S.; Sapkota, N.; Baruwal, P.; Bhattarai, B.; Khanal, K.; & Chapagain, N. P. Field-Aligned Current and Polar Cap Potential and Geomagnetic Disturbances: A Review of Cross-Correlation Analysis. *Earth and Space Science*, **5**(9): 440-455 (2018).
- [3] Adhikari, B.; Baruwal, P.; & Chapagain, N. P. Analysis of supersubstorm events with reference to polar cap potential and polar cap index. *Earth and Space Science*, **4**(1): 2-15 (2017).
- [4] Adhikari, B.; & Chapagain, N. P. Polar cap potential and merging electric field during high intensity long duration continuous auroral activity. *Journal of Nepal Physical Society*, **3**(1): 6-17 (2015).
- [5] Augusto, C. R. A.; Navia, C. E.; de Oliveira, M. N.; Nepomuceno, A. A.; Raulin, J. P. et al. The 2015 summer solstice storm: One of the major geomagnetic storms of solar cycle 24 observed at ground level. *Solar Physics*, **293**(5), 1-28 (2018).
- [6] Adhikari, B.; Chapagain, R.; Sapkota, N. P.; Dahal, N.; & Pandit, D. Daily, seasonal and monthly variation of middle-low latitudes magnetic field during low solar activity. *Discovery*, **53**(255): 181-190 (2017).
- [7] Burgess, D. Collisionless Shocks, in Introduction to Space Physics, edited by M. G. Kivelson and C. T. Russell, Cambridge University Press, Cambridge (1995).
- [8] Chapman, J. F.; & Cairns, I. H. Three-dimensional modeling of Earth's bow shock: Shock shape as a function of Alfvén Mach number. *Journal of Geophysical Research: Space Physics*, **108**(A5): ... (2003).
- [9] Characterization of Saturn's bow shock: Magnetic field observations of quasi-perpendicular shocks A. H. Sulaiman, A. Masters, M. K. Dougherty, *Journal of Geophysical Research: Space Physics*.
- [10] Eriksson, S.; and L. Rastätter. Alfvén Mach number and IMF clock angle dependence of sunward flow channels in the magnetosphere, *Geophys. Res. Lett.*, **40**: 1257–1262 (2013).
- [11] Joshi, N. C.; Bankoti, N. S.; Pande, S.; Pande, B.; & Pandey, K. Behavior of plasma and field parameters and their relationship with geomagnetic indices during intense geomagnetic storms of solar cycle 23. *arXiv preprint arXiv:1003.2868* (2010).
- [12] Kahler, S. W. The role of the big flare syndrome in correlations of solar energetic proton fluxes and associated microwave burst parameters. *Journal of Geophysical Research: Space Physics*, **87**(A5): 3439-3448 (1982).
- [13] Koldobskiy, S.; Raukunen, O.; Vainio, R.; Kovaltsov, G. A.; & Usoskin, I. New reconstruction of event-integrated spectra (spectral fluences) for major solar energetic particle events. *Astronomy & Astrophysics*, **647**: A132 (2021).
- [14] Marcq, S.; Laj, P.; Roger, J. C.; Villani, P.; Sellegri, K. et al. Aerosol optical properties and radiative forcing in the high Himalaya based on measurements at the Nepal Climate Observatory-Pyramid site (5079 m asl). *Atmospheric Chemistry and Physics*, **10**(13): 5859-5872 (2010).
- [15] Matamba, T. M.; & Habarulema, J. B. Ionospheric responses to CME-and CIR-driven geomagnetic storms along 30 E–40 E over the African sector from 2001 to 2015. *Space Weather*, **16**(5): 538-556 (2018).
- [16] Pandya, M.; & Bhaskara, V. Quantitative Assessment of Protons During the Solar Proton Events of September 2017. *Journal of Geophysical Research: Space Physics*, **126**(10): e2021JA029458 (2021).
- [17] Qin, M.; Zhang, X.; Ni, B.; Song, H.; Zou, H.; & Sun, Y. Solar cycle variations of trapped proton flux in the inner radiation belt. *Journal of Geophysical Research: Space Physics*, **119**(12): 9658-9669 (2014).
- [18] Reedy, R. C. Solar proton fluxes since 1956. In *Lunar and Planetary Science Conference Proceedings*, **8**: 825-839 (1977).
- [19] Wiesław, M.; Macek, A. W.; and Beata, K. Intermittent turbulence in the heliosheath and the magnetosheath plasmas based on Voyager and THEMIS data.
- [20] Wu, C. C.; Liou, K.; Lepping, R. P.; Hutting, L.; Plunkett, S. et al. The first super geomagnetic storm of solar cycle 24: "The St. Patrick's day event (17 March 2015)". *Earth, Planets and Space*, **68**(1): 1-12 (2016).